Combustion and Flame 272 (2025) 113907

Contents lists available at ScienceDirect

Combustion and Flame

journal homepage: www.sciencedirect.com/journal/combustion-and-flame

The measurement of turbulent burning velocities of methane-hydrogen-air mixtures at elevated pressures in a spherical vessel

Marwaan Al-Khafaji [a], Junfeng Yang [a,*], Alison S. Tomlin [b], Harvey M. Thompson [a], Gregory de Boer [a], Kexin Liu [c]

[a] School of Mechanical Engineering, University of Leeds, Leeds LS2 9JT, United Kingdom
[b] School of Chemical and Process Engineering, University of Leeds, Leeds LS2 9JT, United Kingdom
[c] Siemens Energy, Lincoln LN6 3AD, United Kingdom

ARTICLE INFO

Keywords:
Turbulent burning velocity
Stretch rate
Flame instability
Methane/hydrogen mixtures
Premixed flame

ABSTRACT

Few previous experimental studies have focused on pre-mixed turbulent burning velocities (u_t) for hydrogen/air and methane/hydrogen/air mixtures, especially at the high-pressure conditions most relevant to gas turbine applications. This work employed a Schlieren technique to measure flame speeds for such mixtures in a spherical stainless steel combustion vessel, from which turbulent burning velocities were derived. The hydrogen volume fractions in methane were 30, 50, 70 and 100%. The initial pressures were 0.1, 0.5 and 1.0 MPa, and the initial temperatures were 303 and 360 K. The equivalence ratio (ϕ) was varied between 0.5 and 2 for pure hydrogen and from 0.8 to 1.2 for methane/hydrogen mixtures. The root mean square (rms) turbulent velocity (u') was varied from 2.0 to 10.0 ms^{-1}. The objectives of this study are: (a) to present an extensive experimental database of turbulent burning velocities for these mixtures over a wide range of conditions; (b) to establish a new correlation for u_t for a flame with Lewis numbers, *Le,* not equal to unity, and (c) to quantify the dependence of turbulent burning velocity on pressure, temperature, stretch rate, laminar flame instability and rms velocity. As the pressure increased, the Taylor length scales decreased, and positive stretch increased, increasing flame wrinkling and u_t. The u_t also increased as the temperature and u' increased. The fuel/air mixture with high laminar flame instability ($Le<1$) has higher u_t than those with higher *Le*. However, the normalised u_t peaked in the region of high laminar burning velocity. This study concluded that the increase in u_t resulting from flame reactivity (laminar burning velocity) is more important than that from positive stretch (negative Ma_b) and flame instability.

1. Introduction

Turbulence's impact on the burning velocities of hydrogen/air and hydrogen/methane/air flames is critical in designing practical engineering devices, such as hydrogen gas turbines. In spherical turbulent pre-mixed flame propagation, the flame front of the initial small flame kernel is affected only by small eddies with high wave numbers that wrinkle the flame surface. Over time, as the flame kernel grows, the flame front becomes increasingly affected by eddies with lower turbulent frequencies, resulting in a continuous increase in turbulent burning velocity [1,2]. To address this effect, the effective root mean square (rms) turbulent velocity u'_k, which represents the local rms turbulent velocity at the flame surface, has been proposed [1]. In this study, and following Bradley et al. [1–4], u'_k is used to analyse turbulent burning velocity for the spherical expanding flame. u'_k accounts for changes in the turbulent power spectrum by integrating the non-dimensional power spectral density over the range of relevant wavelengths.

The turbulent burning velocity (u_t) for any fuel under specific operating conditions is a key determinant in calculating the mass rate of burning. The mass rate of burning depends on the turbulent burning velocity, cold reactant density, and surface area. In the context of this study, u_t determined using a Schlieren technique, is linked to the consumption rate of unburned gases, as Schlieren images rely on changes in mixture density. Bradley et al. [5] concluded that u_t is equal to the engulfment velocity, u_e, at the reference radius, r_v, which falls between r_r (the root of the turbulent flame brush) and r_t (the tip of the flame brush), such that the volume of burned gases inside the sphere matches the volume of unburned gases outside the sphere [5]. They found that the flame radii from Schlieren measurements need to be divided by a factor

* Corresponding author.
E-mail address: J.Yang@leeds.ac.uk (J. Yang).

https://doi.org/10.1016/j.combustflame.2024.113907
Received 16 May 2024; Received in revised form 3 December 2024; Accepted 4 December 2024
Available online 14 December 2024

Nomenclature

A	flame surface area (m^2)
C_p	specific heat (KJ/Kg.K)
D	thermal diffusivity (m^2s^{-1})
Le	Lewis number
L	turbulent integral length scale
Ma_b	flame speed Markstein number
Ma_{sr}	strain Markstein number
P_u	initial pressure (MPa)
P_r	Prandtl number
r_{sch}	flame radius from Schlieren images (mm)
r_v	volumetric flame radius (mm)
u_l	un-stretched laminar burning velocity (ms^{-1})
T_b	adiabatic equilibrium burned gas temperature (K)
T_u	unburned gas temperature (K)
K_{a1}	Karlovitz stretch factor $\left(\frac{\delta_l u_l}{\lambda u'}\right)$
K_a	Karlovitz number $\left(\frac{\delta_l u_l}{\eta u_\eta}\right)$
D_a	Damköhler number
u'	turbulent fluctuation velocity (ms^{-1})
u'_k	the effective root mean square (rms) turbulent velocity (ms^{-1})
u_t	the turbulent burning velocity (ms^{-1})
u_η	the turnover velocity on the Kolmogorov scale, $u_n = u' 15^{0.25} Re_\lambda^{-0.5}$

Greek symbols

δ_l	flame thickness (mm)
k	thermal conductivity (kJ/m.K.s)
μ	dynamic viscosity (kg/m.s)
ν	kinematic viscosity (m^2s^{-1})
φ	equivalence ratio
ρ_b	burned gas density (kg/m^3)
ρ_u	un-burned gas density (kg/m^3)
λ	turbulent Taylor length scale (mm)
η	turbulent Kolmogorov length scale (mm)
Re_λ	Reynolds number based on Taylor length scale
Re_L	Reynolds number based on integral length scale

of 1.11 to obtain r_v, at which the u_t provides the mass burning rate of a turbulent pre-mixed flame.

The turbulent burning velocity is a crucial physical parameter in turbulent combustion, often serving as an input parameter for combustion modelling [6–9]. Consequently, numerous studies have aimed to establish a general correlation for u_t [2,10–14]. These correlations have linked the turbulent burning velocity to both turbulent fluctuation velocity [15] and laminar burning velocity [16,17]. A review of five different u_t correlations was conducted and presented in [12]. The parameters considered in these correlations typically include the laminar burning velocity u_l, flame thickness δ_l, rms velocity u', and integral length scale, L. However, it is worth noting that the predicted values of u_t from these correlations are often inconsistent within themselves and with experimental results, primarily due to the omission of thermo-diffusive effects [12]. In alignment with Damköhler's theory, the turbulent transport of heat and mass within mixtures and the total surface area of wrinkled flamelets stand out as the primary factors governing the turbulent burning velocity [10]. Hence, Bradley et al. [2–4] introduced the *U-K* correlation$\left(U = \alpha K_{a1}{}^{\beta}\right)$, where U is the ratio of the turbulent burning velocity to the effective rms turbulence velocity, and K_{a1} is the Karlovitz stretch factor, which will be presented in the next section. The *U-K* correlation takes into account the influence of chemistry, turbulent length scales, flame thickness, flame stretch rate, and rms turbulence velocity. The constants (α and β) are functions of Ma_{sr}, which incorporates the effect of strain rate on the turbulent burning velocity [2–4]. However, the uncertainty in the Markstein number is high, especially for mixtures of non-unity Lewis number. Markstein number is defined as a Markstein length to flame thickness (δ_l) ratio. The Markstein length determination is very sensitive to the onset of instability, and the δ_l varies based on the calculation method used, as discussed in the authors' previous work [18].

Recently, Wang et al. [13] correlated u_t with differential-diffusion and stretch effects. They used the general scaling law based on the Damköhler hypothesis: $u_t/u_l = f\left((u'/u_l)^{\alpha}, (L/\delta_l)^{\beta}, Le^{\gamma}\right)$, where L is the turbulent integral length scale, δ_l the laminar flame thickness, and *Le* is the Lewis number. The constants α ∼ 0.5–1 and β ∼ 0–0.5 [19], the power exponent (γ) for *Le,* have a negligible effect on the correlation for u_t/u_l due to the small absolute value of *Le* in comparison to R_e [13]. The present study investigates the scaling parameters of previous studies [2–4,13] to correlate the turbulent burning velocity for pure hydrogen/air and methane/hydrogen/air mixtures at high initial pressure and rms turbulent flow velocity.

Few previous experimental studies have considered turbulent burning velocities for hydrogen and methane/hydrogen mixtures, particularly at the high-pressure conditions most relevant to gas turbine applications. Goulier et al. [14] and Morones et al. [20] conducted experimental investigations of turbulent expanding flames of lean hydrogen/air mixtures at atmospheric pressure, with turbulent fluctuation velocities ranging from 1.0 to 2.8 ms^{-1}. The turbulent burning velocities of methane/hydrogen/air mixtures have been studied over a broad range of initial rms velocities u' in [21], but solely at low pressure (0.1 MPa) and with a hydrogen volume fraction up to only 50%. Other studies that explored turbulent flames of H_2/CH_4 air mixtures [22–25] focussed on only a limited range of hydrogen fractions, pressures and equivalence ratios. Therefore, the novelty of the present study is to investigate the turbulent flame propagation for hydrogen/air and methane/hydrogen/air mixtures at high pressure (0.1 MPa) and high rms velocities (u'= 2–10 ms^{-1}), which are most relevant to hydrogen-fuelled ICEs and industrial gas turbines and burners. Moreover, this study revisited the previous U/K diagram and plotted new data. The latest data is situated in the regime considered unstable in earlier studies [2–4]. In addition, this study provided a new *U-K* correlation based on Ma_b instead of Ma_{sr}.

The objectives of the study are threefold: (a) the measurement of turbulent burning velocities of methane/hydrogen/air and pure hydrogen-air mixtures under elevated pressure conditions, thereby providing an extensive experimental database for these mixtures across a wide range of conditions; (b) creating a novel u_t correlation that encompasses all parameters that influence turbulent burning velocity [2,3,13,15,16,26,27]; and (c) quantifying the dependence of turbulent burning velocity on pressure, temperature, stretch rate, laminar flame instability and rms velocity. The paper is organised as follows: Section 2 outlines the experimental methods and apparatus setup, while Section 3 presents the primary experimental results and the ensuing discussion. Conclusions are drawn in Section 4.

2. Research methodology

The present study investigates turbulent burning velocities for methane/hydrogen/air mixtures with hydrogen volume fractions of 30%, 50%, 70%, and 100% across a much broader spectrum of pressures than previous work, including 0.1, 0.5, and 1.0 MPa. Equivalence ratios

varied between 0.8 and 1.2 for H_2/CH_4/air mixtures and 0.5 and 2 for pure H_2/air. Additionally, u' was adjusted within the 2 to 10 ms^{-1} range. More information about the experimental conditions used within the present study is given in the supplementary material (SM).

2.1. Experimental methods and apparatus setup

The mixture preparation and experimental procedures for using the Leeds MK-II fan-stirred combustion vessel and auxiliary systems were detailed in [18], which focused on the laminar flame propagation of hydrogen-methane-air mixtures. For investigating the turbulent flame propagation, the rotating speed of four stirred-fans, f, was adjusted for the desired u', using the following equation described in [28]:

$$u' = 0.00124\, f \tag{1}$$

where f is the fan speed in rpm. The values of u' in the Leeds MK-II vessel have been studied comprehensively using a range of flow measurement techniques, including Hotwire Anemometry (HWA) [3], Laser Doppler Velocimetry (LDV) and Particle Image Velocimetry (PIV) [3,12,28]. Throughout the experiments, the fans operated at a constant speed. It is assumed that u' and the integral length scale, L, are independent of pressure and temperature. The validity of this assumption has been demonstrated previously [2,5,28]. The reference flame radius is measured using the Schlieren radius 'r_{sch}' to obtain the reference radius, r_v, as described in [5]. The u_t, is then determined via the mass conservation equation [2,3,5,29]:

$$u_t = 0.9\,(\rho_b/\rho_u)\frac{dr_{sch}}{dt} \tag{2}$$

where ρ_u is the unburned gas density at initial gas temperature (T_u) and ρ_b is the burned gas density at adiabatic temperature (T_b), assuming that the flame is adiabatic [30–32]. The time step (dt) is calculated as 1/(camera frame rate). The chemical equilibrium program, GASEQ [33] was employed for calculating the gas properties at the specified temperature, pressure and equivalence ratios.

2.2. Turbulent flow and flame characteristic/field definitions

The laminar burning velocity (u_l) and Markstein number (Ma_b) of hydrogen-methane-air mixtures used in this work were taken from previous measurements [18]. The value of the integral length scale in the MK-II vessel is 20 mm, as discussed above. The Taylor- and Kolmogorov- length scales, λ and η, were derived using respectively:

$$\frac{\lambda}{L} = \frac{A}{Re_\lambda} \tag{3}$$

$$\eta = \frac{\lambda}{15^{0.25} Re_\lambda^{0.5}} \tag{4}$$

where Re_λ is Reynolds number based on the Taylor length scale.

$$Re_\lambda = \frac{u'\lambda}{\upsilon} \tag{5}$$

υ is the unburned kinematic viscosity and A is a constant (A= 16 ±1.5 [12,34]). The turbulent time scale is the ratio of turbulent length scale to u'. The chemical time scale is the ratio of the flame thickness δ_l to the laminar burning velocity u_l [35,36].

The Karlovitz stretch factor K_{a1}, which is the ratio of chemical time scale to the turbulent time scale [37], is calculated as in [2]:

$$K_{a1} = \left(\frac{u'}{\lambda}\right) \Big/ \left(\frac{u_l}{\delta_l}\right) \tag{6}$$

where u'/λ is the rms strain rate, with $Re_\lambda = 4(Re_L)^{0.5}$, $\delta_l = \left(\frac{\upsilon}{u_l}\right)/Pr$, and $Re_L = \frac{L\,u'}{\upsilon}$. Thus, the Karlovitz stretch factor K_{a1} in this study is calculated by:

$$K_{a1} = 0.25\left(\frac{1}{Pr}\right)(u'/u_l)^2 (Re_L)^{-0.5} \tag{7}$$

In [2], the assumption of a Prandtl number (Pr) of 1 was made, although this assumption is not practical when dealing with high hydrogen volume fractions. As the hydrogen fraction increases, the thermal diffusivity also increases, leading to a decrease in Pr. Additionally, Pr decreases with increasing ϕ when the hydrogen content in the fuel/air mixture rises. In the present study, the Prandtl number is calculated as the ratio of kinematic viscosity to thermal diffusivity (υ/α).

During the propagation of the turbulent spherical expanding flame, the effective rms velocity continuously increases, leading to increases in the burning velocity. Therefore, unlike laminar flames, there is no single u_t, which varies with the flame radius. Following the studies of Bradley et al. and Lawes et al. [5,12], u_t at a flame radius of 30 mm was chosen for the analysis of this study since positioning the flame at this radius places it beyond the influence of the spark plasma, as the spark effect typically extends up to 10 mm [24]. In addition, the flame at 30 mm is exposed to the full range of turbulent scales, as the flame kernel exceeds the vessel's integral length scale (L = 20 mm) [3,14,28], and the turbulent flow in this region is homogenous and isentropic [28]. The method of deriving the effective rms velocity (u'_k) is presented in the SM.

3. Results and discussion

3.1. Turbulence regimes

Various regimes have been used to describe how turbulent pre-mixed flames depend on the most influential parameters [36,38,39]. These encompass both chemical scales (such as u_l and δ_l) and turbulent scales (including L, λ, η, and u'). The integral scales primarily govern flame convection and can only induce significant wrinkling in large flame kernels [1,12]. In contrast, the Kolmogorov scales may lack the requisite energy for effective flame wrinkling [39]. Therefore, the Taylor scales assume a central role in flame wrinkling due to their responsibility for shear forces. The λ scale increases as the temperature rises, while it decreases as the pressure and fan speeds (u') increase. The λ and η length scales are presented in the SM.

Fig. 1a, b depict the experimental conditions and turbulence parameters outlined within the regime proposed in [36,38,39]. The Y-axis represents the wrinkling factor (u'/u_l), while the X-axis denotes the size of the wrinkling (L/δ_l). The lines in this diagram represent constant values for Reynolds number (Re), Karlovitz number (K_a), Damköhler number (Da) and the effective turbulent length scale (l_s). According to the Klimov-Williams criteria, nearly all flames with 30% H_2, and some with 50% and 70% H_2 (those at high initial pressure), fall within the reaction sheet regime ($K_a > 1$), primarily due to their low laminar burning velocity and, consequently, an extended chemical time scale. However, these flames may not experience disturbances at the Kolmogorov scale (η), as these lack the requisite momentum for effective mass and heat transfer in and out of the preheat zone [11].

This assessment is consistent with the criteria established by Poinsot et al. [38] and Pope [39], as indicated by the line $\delta_l = l_s = 13\eta$. Consequently, all experiments fall below this line, signifying the existence of flamelets for all experimental conditions. The flamelet assumption is valid in both the wrinkled and corrugated flamelet regimes, where chemical reactions occur significantly faster than turbulent mixing [40]. Some experiments with 100% H_2 fall within the wrinkled flamelet regime, primarily due to the high laminar burning velocity. Pure hydrogen exhibits a short chemical time scale and a thin flame structure. Consequently, K_a decreases as u'/u_l decreases and L/δ_l increases. This suggests that the flame surface for pure hydrogen

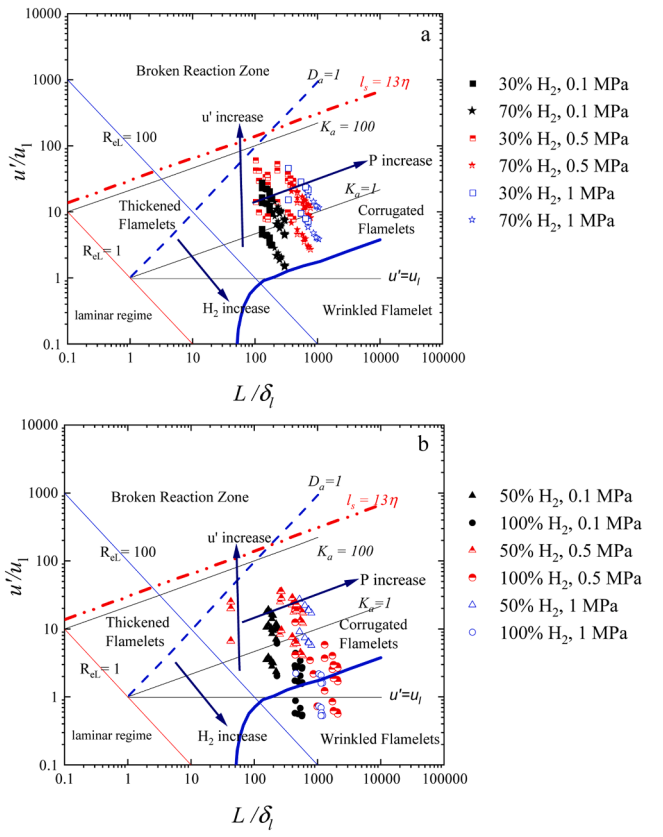

Fig. 1. Regime diagram [11,38,39], with the present experimental conditions, with laminar burning velocity and flame thickness taken from [27]. The legends for the present experimental conditions and turbulence parameters represent (a) 30, 70% H_2 and (b) 50, 100% H_2. ϕ ϵ[0.8 1.2] for mixtures with 30%,50% and 70% H_2; [0.5 2] for pure H_2.

exhibits laminar-like propagation (i.e. a spherical flame) with large-scale wrinkles, as will be discussed in the following section.

3.2. Turbulent flame radius and flame images

Fig. 2 illustrates the time history of the flame radius (r_v) for methane-hydrogen mixtures with various u' at 0.5 MPa, 360K and $\phi = 1$. In all these experiments, the r_v-time curves exhibit an upward concave shape, signifying flame acceleration over time. Flame propagation speed increases with greater hydrogen volume fractions and higher fan speeds,

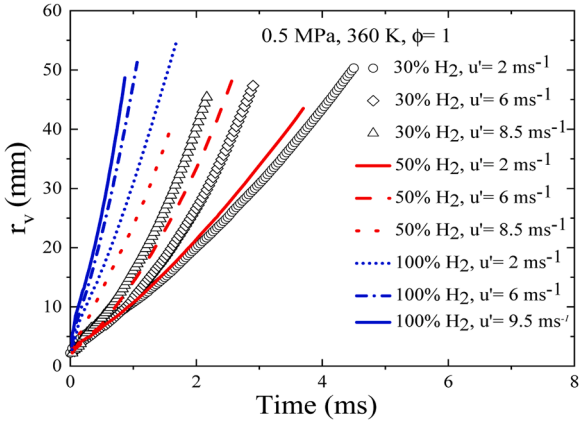

Fig. 2. The equivalent flame radius vs. time for stoichiometric mixtures at 0.5 MPa and 360 K.

u'. For instance, at $u' = 2$ ms^{-1}, the flame reaches the optical field of view's limits ($r_v = 55$ mm) after 5 ms for 30% H_2, whereas it takes approximately 3.5 ms for 100% H_2. Notably, the maximum flame radius varies with the fan speed/u'. The maximum flame radius is achieved at the lowest fan speed/u', measuring around 55 mm for $u' = 2.0$ ms^{-1}, while it falls within the range of 37 mm (50% H_2) to 47 mm (100% H_2) at higher fan speeds. At high fan speeds, large turbulent eddies cause erratic displacement of the small flame kernel during the early stages of flame propagation, as depicted in Fig. 3a & b. Consequently, the flame reaches the optical field of view's limits before further development can occur. At high fan speeds, the flame drift is more prominent at lower H_2 volume fractions than at higher H_2 volume fractions. A comparison between Fig. 3b & c shows that the flame drifts to the left for 50% H_2, while it remains centred for 100% H_2 with a high fan speed ($u' = 9.5$ ms^{-1}). The increase in H_2 fraction leads to reduced chemical time scales, causing the flame to develop before large turbulent eddies have a significant impact. Referring back to the regime diagram (Fig. 1b), the pure hydrogen flame is situated within the wrinkled flamelets regime, indicating that hydrogen flame propagation exhibits a spherical flame with a wrinkled surface (Fig. 3c).

For a fixed fuel/air mixture, initial temperature, and u', an increase in pressure has three primary effects: (i) Taylor length scales decrease, (ii) Markstein length decreases, indicating a positive stretch rate effect on the flame speed, and (iii) the mixture reactivity decreases, as indicated by a lower laminar burning velocity u_l, allowing for more time for the flame to be wrinkled by the turbulent scales and (iv) the Darrieus–Landau (DL) instability is enhanced due to the smaller flame thickness. Therefore, a reduction in Taylor scales imposes a positive stretch on the flame. While the stretch effect can be quantified using the Markstein number (Ma_b) [2,11,18], in this scenario, flame wrinkling results from the combined influences of stretch, chemical, turbulent scales and instability effects. Consequently, the finest flame wrinkling scales are observed at the highest pressure. Low Ma_b values, extensive chemical time scales, reduced Taylor eddies, and flame thicknesses collectively contribute to finer flame wrinkling. This effect is also noticeable at fixed u'_k, P_u, T_u, and ϕ (Fig. 4a–d). As the hydrogen volume fraction increases, both Ma_b and u_l increase, leading to larger flame wrinkling scales. A clear distinction can be observed when comparing the images for 30% H_2 (with more condensed scales) and 100% H_2 (with less condensed scales). In the case of 30% H_2, turbulent eddies have more time to create surface wrinkles, thanks to the longer chemical lifetime of the flame [12]. The flame with 30% H_2 falls into the thickened flamelet regime with fine surface scales, while the flame with 100% H_2 situates in the wrinkled flamelet regime (Fig. 1a & b). Moreover, an increase in u' leads to a reduction in λ, resulting in smaller flame wrinkling scales. Flame wrinkling is also observed at different times after ignition in the same experiment. The flame at $r_v = 12$ mm exhibits larger scales than the flame at $r_v = 40$ mm. The proportion of affected eddies increases as the flame kernel expands [1]. This phenomenon has been quantified in terms of an increasing effective rms velocity, u'_k, as the flame radius increases.

It is very challenging to qualitatively assess the effect of stretch on flame wrinkling, as this is interacts with the effect of the thermal diffusive (TD) and DL instability. The flame images for 100% H_2 at $T_u =$ 360 K, $r_v = 40$ mm, and $u' = 2$ ms^{-1} are presented in Fig. 5a–d. Both chemical and turbulent scales are held constant to investigate the stretch effect on the turbulent flame. In Fig. 5a, b, there is an 8% difference in the laminar burning velocity for these cases, while in Fig. 5c, d, the difference is 6%. The sole parameter that changes is Ma_b, which is 25.6 for $\phi = 1.5$, 19.6 for $\phi = 2$ at 0.1 MPa, and -22.7 for $\phi = 1$, -10.5 for $\phi =$ 2.5 at 0.5 MPa. However, flame thickness decreases with pressure, which enhances the DL instability. Flames with lower Ma_b values allow for more wrinkling, but these differences can be difficult to identify. This difficulty arises from the need to achieve a large change in Ma_b, and a transition from positive to negative Ma_b, while keeping the laminar burning velocity and flame thickness constant. Such a transition is not

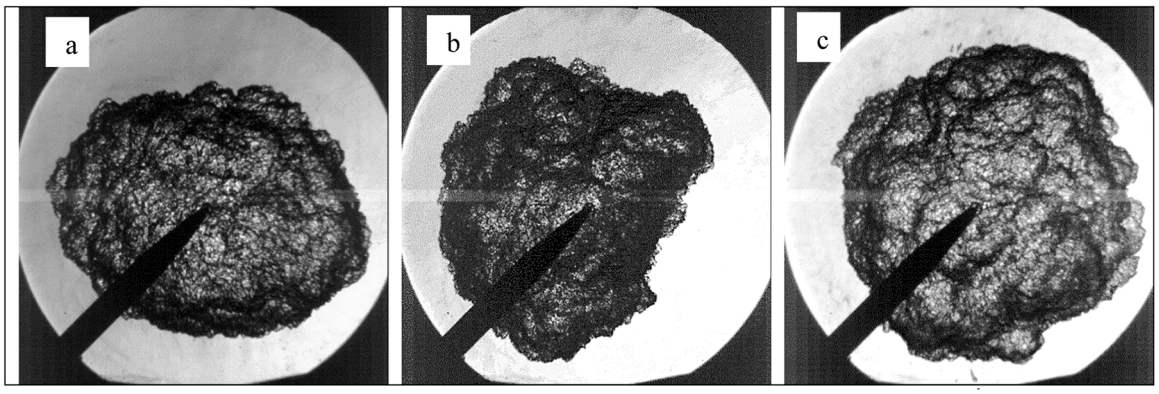

Fig. 3. Flame images, P_u = 0.5 MPa, T_u= 360 K and ϕ =0.8, (a) 50% H_2, u'= 2 ms^{-1}, (b) 50% H_2, u'= 8.5 ms^{-1} and (c) 100% H_2, u'= 9.5 ms^{-1}.

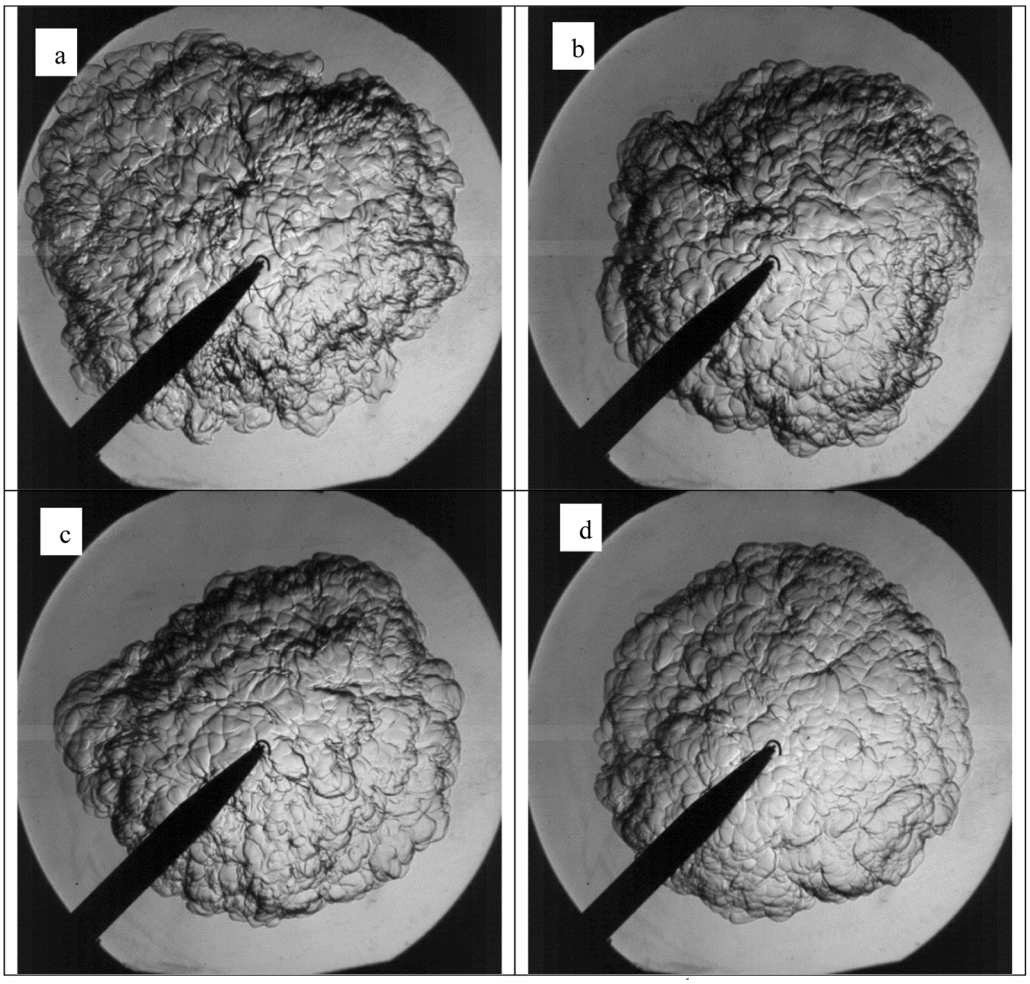

Fig. 4. Flame images at r_v= 45 mm, 0.1 MPa, 360 K, u'= *2* ms^{-1} and ϕ= 1, (a) 30% H_2, Ma_b= 4.1, (b) 50% H_2, Ma_b= 5.4, (c) 70% H_2, Ma_b= 9.65 and (d) 100% H_2, Ma_b= 25.2.

feasible under the current conditions. The effect of stretch on the turbulent burning velocity will be addressed in the following sections.

3.3. Turbulent burning velocity u_t

Eq. (2) is employed to calculate u_t. Figs. 6 and 7 depict u_t as a function of the flame radius, r_v, for various CH_4/H_2/air mixtures, pressures, and u' values. Initially, the turbulent burning velocity is relatively slow at the onset of the explosion, gradually increasing as the flame develops. This behaviour has been previously explained [1]: when the flame initiates from the central ignition source, the flame surface can only be wrinkled by eddies with length scales smaller than the size of the flame kernel. This implies that the effective rms turbulent velocity (u'_k), which is measured in the absence of the flame, is smaller in the centre and increases toward the vessel wall until it reaches the value of u'. In other words, the proportion of turbulent eddies affecting the flame grows as the flame kernel expands [1–3]. Consequently, spherical turbulent flame experiments provide data for turbulent burning velocities over a range

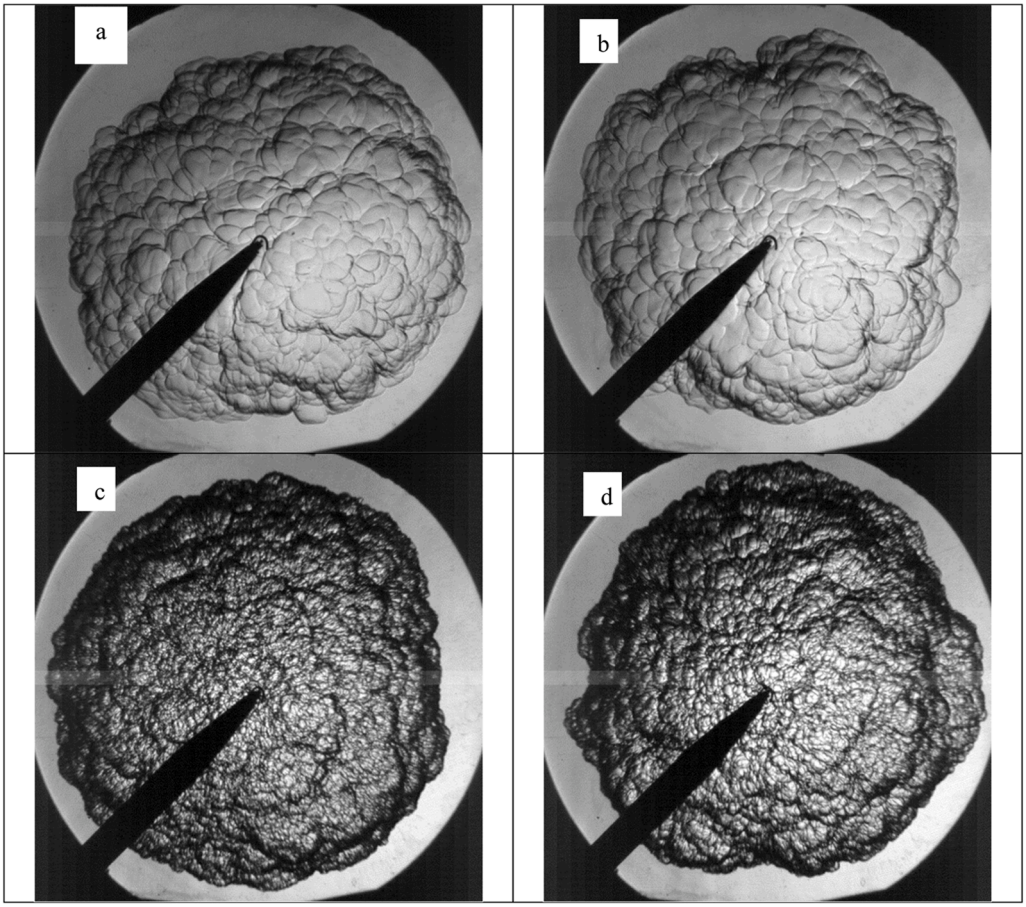

Fig. 5. Flame images for 100% H_2 at T_u= 360K, r_v= 40 mm, and u'= 2 ms^{-1} (a) P_u= 0.1 MPa, Ma_b= 25.6, ϕ= 1.5, u_l= 3.68 ms^{-1}, (b) P_u= 0.1 MPa, Ma_b= 19.6, ϕ= 2 u_l= 3.55 ms^{-1}, (c) P_u= 0.5 MPa, Ma_b= -22.7, ϕ= 1, u_l= 2.35 ms^{-1}, (d) P_u= 0.5 MPa, Ma_b= -10.5, ϕ= 2.5, u_l= 2.75 ms^{-1}.

of turbulent scales [20]. Fig. 8 illustrates the relationship between u_t and u'_k, showing that u_t increases linearly with u'_k. In each explosion, the maximum u_t is observed at the maximum u'_k, as u'_k approaches u'. This pattern is consistently observed across all conditions, and additional plots for u_t-u'_k relationships are available in the SM.

It is widely recognised that elevated pressures reduce the burning rate in laminar explosions due to the promotion of chain-terminating reactions [18,41]. However, for mild turbulent conditions, such as u' = 2 ms^{-1} in Fig. 6, u_t of the CH_4/H_2 mixture remains relatively constant as the initial pressure is increased from low (0.1 MPa) to high (1 MPa). In the case of 30% H_2 with ϕ= 0.9, at $u' \geq$ 6 ms^{-1}, u_t increases by approximately 15% as the pressure increases from 0.1 to 0.5 MPa and by approximately 10% as the pressure increases from 0.5 to 1 MPa. Similarly, for 70% H_2 at high u' = 6 ms^{-1} and ϕ= 1.2, u_t remains relatively unchanged as the pressure is increased from 0.5 to 1 MPa. As mentioned earlier, the increase in pressure results in (i) positive flame stretch, (ii) a reduction in Taylor length scales, (iii) a decrease in the flame reactivity, i.e., the laminar burning velocity (u_l) and (iv) enhancement in the DL instability due to the sharp density gradient across the flame front due to the reduced ratio of laminar flame thickness to the global flame size [13]. These effects collectively lead to a finer, more wrinkled flame structure, which in turn increases the turbulent burning velocity [12]. When comparing Fig. 7a and b at u' = 6 ms^{-1}, its apparent that u_t increases as the pressure increases from 0.5 to 1 MPa for lean mixtures, while there is no significant change for rich mixtures. This can be attributed to the DT instability as Lewis number, *Le*, < 1 with lean mixtures and ≥1 for rich mixtures [42]. The increase in pressure results in a finer flame structure but with lower flame reactivity (u_l). Additionally, the interaction between the turbulent flow and flame is contingent upon the flame's dependence on the stretch rate. This can be inferred from the fact that Ma_b for lean hydrogen is lower than that for rich hydrogen [18]. Changing the pressure leads to alterations in both chemical and turbulent time scales along with the Markstein number and flame instabilities.

The effect of flame stretch and the DL and TD flame instabilities can be quantified while keeping the chemical and turbulent scales constant, as illustrated in Fig. 9. Ma_b decreases from -10.5 to -22.7 and *Le* increases from ~1.1 to ~ 1.8 as ϕ increases from 1 to 2.5 while u' is held constant. For ϕ= 2.5, u_l is 14% higher than u_l at ϕ= 1 [18]. However, u_t for ϕ= 2.5 is approximately 20% lower than u_t at ϕ= 1. This is due to both, the stretch (Ma_b) and laminar flame instabilities (*Le*) effect. This trend has also been observed in previous studies, where fuels with positive stretch (negative Ma_b) were found to burn faster in turbulent spherical flames than those with negative stretch (positive Ma_b) [2,43,44]. Moreover, the mixture with high laminar flame cellularity (lower *Le*) has more turbulent flame wrinkling than the mixture with low laminar flame cellularity (higher *Le*) [13].

The turbulent burning velocities at a volumetric flame radius of 30 mm are depicted as functions of equivalence ratio in Figs. 10 and 11, including all experimental conditions. The corresponding effective rms velocity, u'_k at 30 mm is given in Table 1. In these figures, it is evident that u_t increases with the hydrogen fraction, u'_k, and initial temperature. Moreover, higher u' values reduce λ, resulting in more flame wrinkling. Pressure has an interesting effect: u_t remains relatively constant at low fan speeds (u' = 2 ms^{-1}) but increases with pressure at $u' \geq$ 6 ms^{-1}, as discussed earlier. As the equivalence ratio changes, u_t varies and peaks at lean conditions for H_2/CH_4 and rich conditions for pure H_2 flames. This variation can be attributed to modifications in flame reactivity, flame

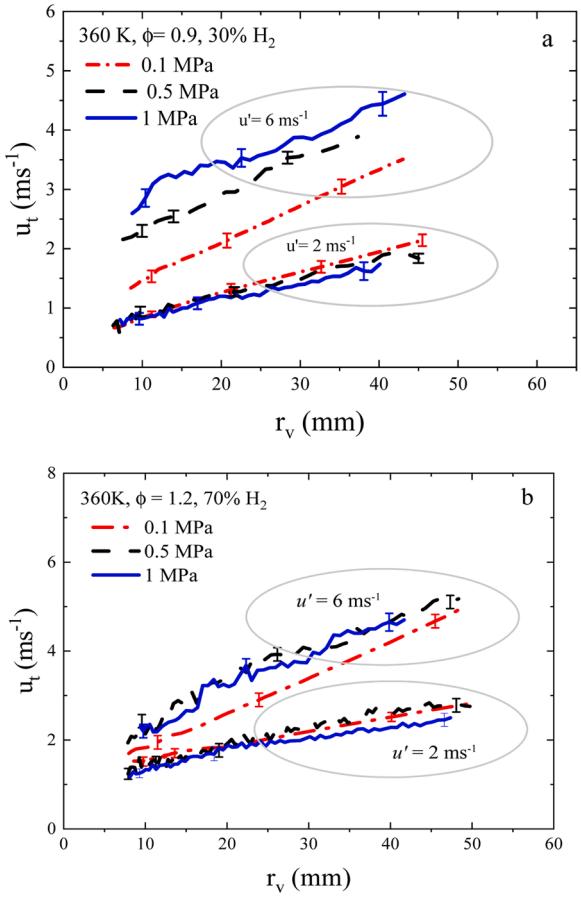

Fig. 6. The variation of turbulent burning velocity with the flame radius for CH_4/H_2/air mixtures at different pressures and initial rms velocities, (a) 30% H_2, ϕ=0.9 and (b) 70% H_2, ϕ= 1.2.

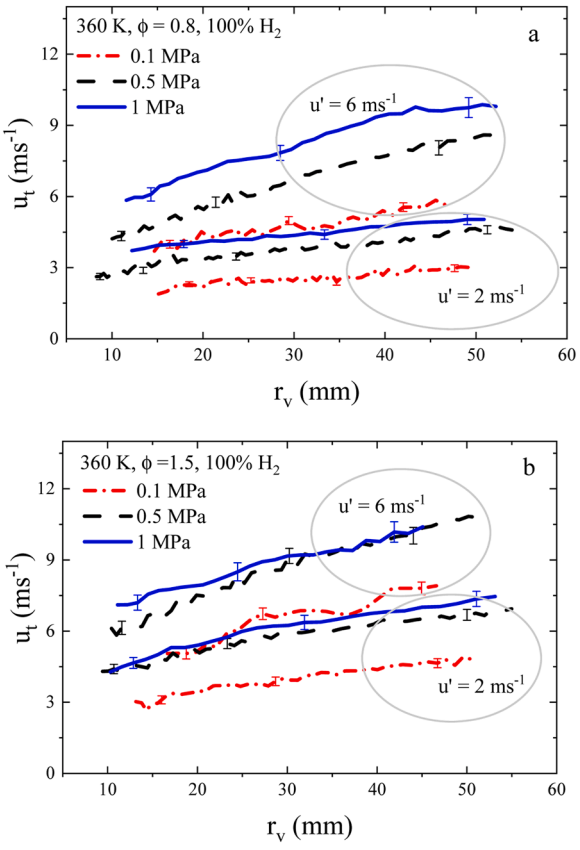

Fig. 7. The variation of turbulent burning velocity with the flame radius for H_2/air mixtures at different pressures and initial rms velocities, (a) ϕ=0.8 and (b) ϕ= 1.5.

thickness, and flame stretch rate (u_l and Ma_b) [4,11]. The maximum u_t for H_2/CH_4 mixtures occurs on the lean side (ϕ= 0.9 – 1.0). Notably, Ma_b and *Le* are lower on the lean side than on the rich side, despite higher u_l as discussed in Fig. 9. Conversely, for most pure H_2 flames, the maximum u_t appears on the rich side (ϕ= 1.7). This is observed even though Ma_b and *Le* are lower on the lean side. It is important to note that u_l at ϕ= 1.7 is 8–10 times higher than at ϕ= 0.5. For H_2/CH_4/air mixtures, the stretch and laminar flame instability effects dominate the flame reactivity since the change in u_l is relatively small (≤ 20%) when ϕ varies from 0.8 to 1.2. In contrast, in pure H_2 flames, flame reactivity takes precedence over the stretch and cellularity effects.

3.4. *Effect of flame stretch rate and flame instabilities on turbulent burning velocity*

In the flamelet regime, the localised flame propagation speed can be significantly influenced by flame stretch rates, potentially leading to flame extinction. This underscores the importance of quantifying the effect of stretch on turbulent pre-mixed flames. The laminar flamelet model for interpreting turbulent pre-mixed flames suggests that the influence of stretch rates depends on the Lewis number, *Le*. The Markstein number, Ma_b, is a parameter that can be experimentally measured and represents the effect of the Lewis number [2]. It has been reported in the literature that mixtures with $Le < 1$, signifying the presence of the DT instability, burn faster than those with $Le > 1$ [13,45]. Another observation in the literature is that laminar flamelets subjected to positive stretch rates with $Le < 1.0$ and negative Ma_b values, experience an increase in turbulent burning velocity, while u_t is slower for mixtures with $Le > 1.0$ and positive Ma_b values [12].

To quantify the effect of stretch on u_t, it is normalised by u_l to mitigate the influence of chemical scales and is plotted as a function of Ma_b in Fig. 12. In this context, both chemical and turbulent length scales must be held constant to investigate the impact of flame stretch and flame instabilities. At fixed u' and pressure, the normalised u_t increases in the negative range of Ma_b (low *Le*) but decreases as Ma_b becomes more negative. For instance, in the case of 50% H_2, the peak value of the normalised u_t occurs in the range of $-10 < Ma_b < -5$, while for 100% H_2, it peaks in the range of $-16 < Ma_b < -14$ and the curves are flattened in the most negative regime. This is attributed to the fact that laminar burning velocity significantly influences the turbulent burning velocity in this region. In the case of pure H_2, the most negative Ma_b is associated with the lean side, where u_l at ϕ= 1.7 is 8–10 times that at ϕ= 0.5. This demonstrates that the effect of chemical time scales dominates the effects of stretch and flame instability in pure H_2 flames. The flames here are in the wrinkled flamelet regime (Fig. 1), where the impact of turbulent eddies is not large enough to compete with the advancement of the flame front due to the high laminar burning velocity. Hence, in this region, laminar flame propagation dominates over the corrugation of the flame front by turbulence. It can also be stated that the claim that positive stretch (negative Ma_b) increases the turbulent burning velocity is not universally valid.

The influence of stretch can also be examined using the classical *U-K* diagram [4], to which the present data has been added, as shown in Fig. 13. In this diagram, the y-axis represents *U*, which is u_t/u'_k, while the x-axis represents the Karlovitz stretch factor (K_{a1}), and the numbers adjacent to the black solid lines represent values of Ma_{sr} from [4]. This diagram, initially developed in [2,3], clearly illustrates the effect of stretch on turbulent burning velocity and its potential to lead to flame extinction. The regime under Ma_{sr}=5 is recognised as the flame extinction regime [4]. Notably, none of the present experiments fall

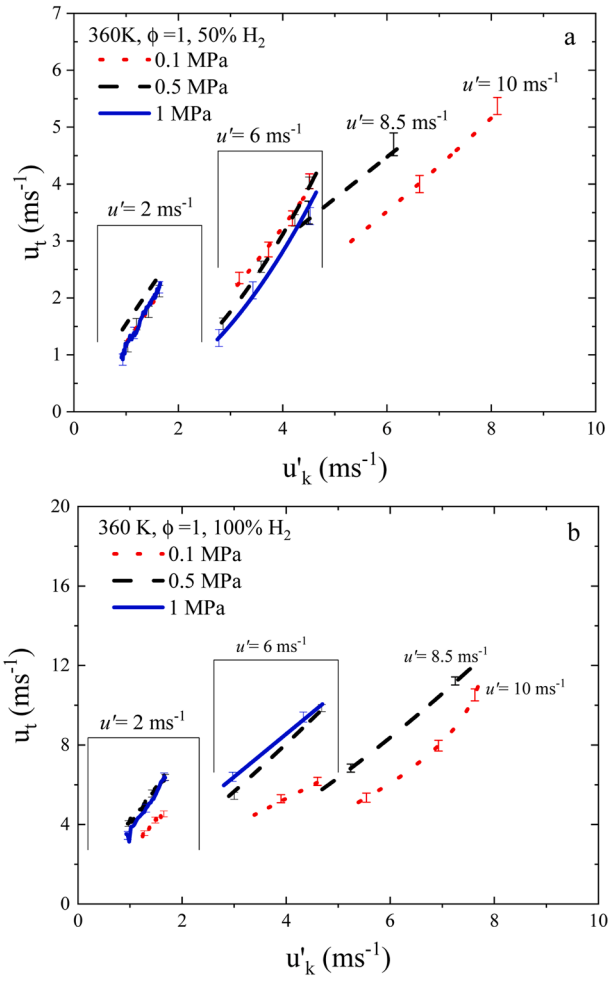

Fig. 8. Variation of turbulent burning velocity u_t with the effective rms velocity u'_k for different mixtures, pressures and initial rms velocities u' with ϕ = 1 and T=360, (a) 50% H_2 and (b) 100% H_2.

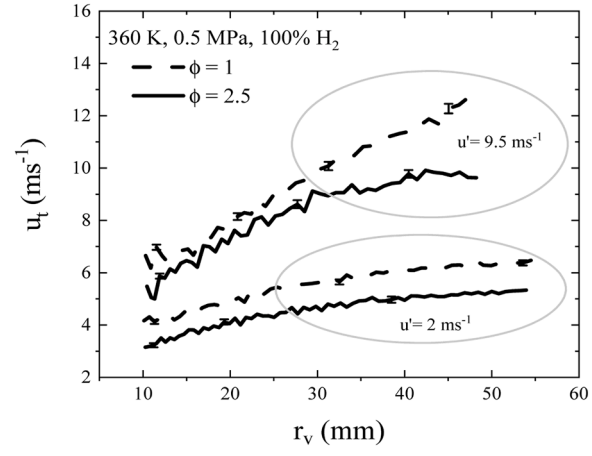

Fig. 9. Variation of turbulent burning velocity with the flame radius for H_2/air mixtures at 360 K, 0.5 MPa and initial rms velocities. For ϕ= 1, Ma_b= -22.7 and u_l= 2.35 ms^{-1}. For ϕ= 2.5, Ma_b= -10.5, u_l= 2.75 ms^{-1}.

within this regime, owing to the increased flame resistance to strain-induced extinction due to the addition of hydrogen [46,47].

Nevertheless, experiments involving hydrogen volume fractions of 50% or less at 303 K are closer to the flame extinction regime than those with 70% or higher. Flame extinction was observed with 30% H_2, 303 K, $\phi \geq 1.1$, and $u' \geq 6$ ms^{-1}. This could be due to the low flame reactivity (low u_l) and the elevated heat loss linked to the lower fresh gas temperature. It is worth noting that flame extinction was not observed under the same conditions with an initial temperature of 360 K. Additionally, more than half of the present measurements are in the region with $K_{a1} \leq 0.1$, and most of the data for pure H_2 falls within the region of $K_{a1} \leq 0.01$. As discussed previously, the increased H_2 fraction leads to higher u_l and reduced flame thickness, resulting in low K_{a1} values. In reference to the regime diagram, explosions with 100% H_2 are in the flamelet regime, as $K_{a1} << 1$. The flames in the low K_{a1} region exhibit high U values. According to Bradley et al. [2], the high normalised turbulent velocity in the low K_{a1} region is attributed to stretch and flame instability effects. However, it is important to consider the chemical time scale (u_l) when analysing the stretch effect, as discussed in relation to Fig. 12. Therefore, this study suggests that the high turbulent velocity values in hydrogen flames primarily result from the high flame reactivity.

3.5. Turbulent burning velocity correlation

The turbulent burning velocity is a crucial physical parameter in turbulent combustion, often serving as an input parameter for combustion modelling [6–9]. Different scaling parameters have been used to correlate u_t/u' and u_t/u_l by considering the effect of flame stretch, Lewis number, turbulent length scales and pressure [13]. The primary factors governing the turbulent burning velocity are the turbulent transport of heat and mass within mixtures, the chemical time scales (u_l and δ_l), flame stretch rate and the total surface area of wrinkled flamelets which is associated with turbulent flow intensity and pressure.

Based on the literature review, the best performance is obtained from two correlations: (i) U-K_{a1} correlation [2–4] and (ii) the general scaling law $u_t/u_l = f\left((u'/u_l)^{\alpha}, (L/\delta_l)^{\beta}, Le^{\gamma}\right)$ [13]. The present study focussed on these correlations presented in the current section.

The U-K correlation [2–4] allows the turbulent burning velocity to be correlated under the current fuel and operational conditions.

$$U = u_t/u'_k = \alpha K_{a1}{}^{\beta} \tag{8}$$

The Karlovitz stretch factor (K_{a1}) is given in Eq. (7). The constants (α and β) in Eq. (8) are functions of Markstein number (Ma_b), which account for the effects of Le, curvature stretch, and strain rates [43]. This is the main difference between the present and previous correlations [2–4]. Ma_{sr} is based on previous studies [48–50] that emphasised the sensitivity of turbulent burning velocity to strain rate, making curvature stretch less significant, enabling it to be neglected. However, recent DNS research on lean pre-mixed hydrogen flames [51] has indicated that the effect of curvature stretch on turbulent burning velocity is more substantial than previously thought. Moreover, the method used to evaluate Ma_{sr} was built on the assumption that Le=1 is unsuitable for the current fuel/air pre-mixed flames [52]. Therefore, the present study correlated α and β as a function of Ma_b to include the curvature and strain effects [52,53]. Moreover, Ma_b is a strong function of Le [3,11], which has been shown to have an appreciable effect on the turbulent burning velocity, as discussed earlier and presented in the literature [13,14].

$U = u_t/u'_k$ is plotted as a function of K_{a1} in Fig. 14a–c for different values of the fuel mixture and Ma_b. The current fuel mixtures are classified into groups based on K_{a1} and Ma_b to improve the accuracy of the u_t correlation. Since pure hydrogen flames have low K_{a1} values ranging from 0–0.1, the hydrogen correlation is separated from the CH_4/H_2 one. Fig. 14a shows the pure hydrogen plot with negative and positive Ma_b. The U value for pure hydrogen increases as K_{a1} decreases. In very small K_{a1} ranging between 0 and 0.01, the U value sharply increases. Two correlations for hydrogen flames are presented in Eq. (9) for negative or positive Ma_b values. For higher K_{a1}, two correlations are presented in Eq. (10) for negative and positive Ma_b. The correlation coefficient R^2 values

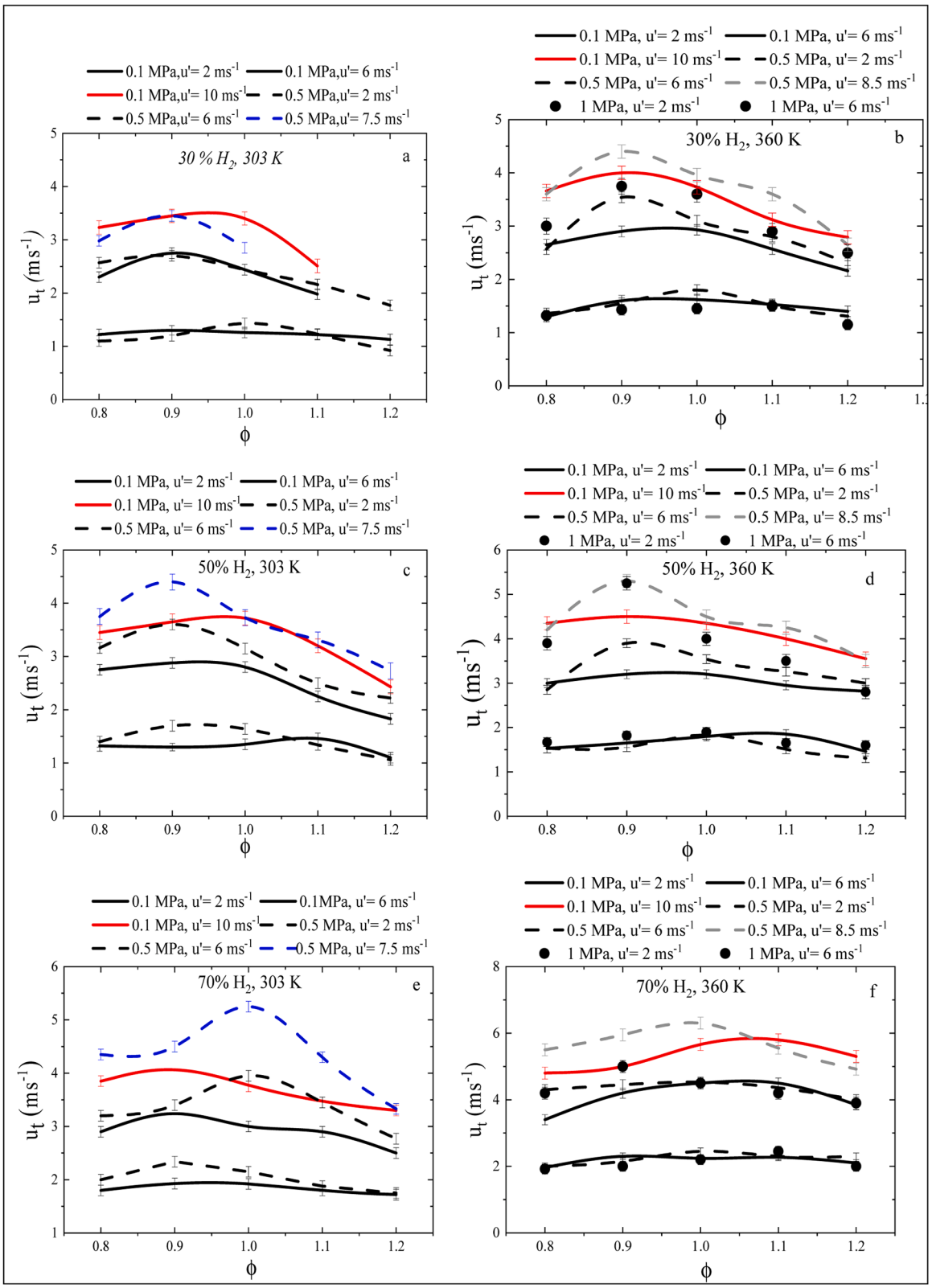

Fig. 10. Variation of turbulent burning velocity at r_v= 30 mm with equivalence ratio for different fuel mixtures, pressures, temperatures and initial rms velocities.

for the above expressions ranged between 0.7 and 0.8. The *U-K* correlation can be recast to $u_t/u' = f\left((u'/u_l)^A, (\lambda/\delta_l)^B\right)$ to match the Damköhler hypothesis. Note that the effect of *Le* is included in the constants A and B as they are functions of Ma_b.

It is important to note the following points about this correlation: (a) it has a low sensitivity to Ma_b, and as a result, the effect of the large error bar in Ma_b on the correlation performance is minimised (b) it is valid for the u_t measured on the reference radii r_v around which the volume of the unburned gases equals the volume of the burned gases (changing this reference would require the correlation to be modified), (c) the

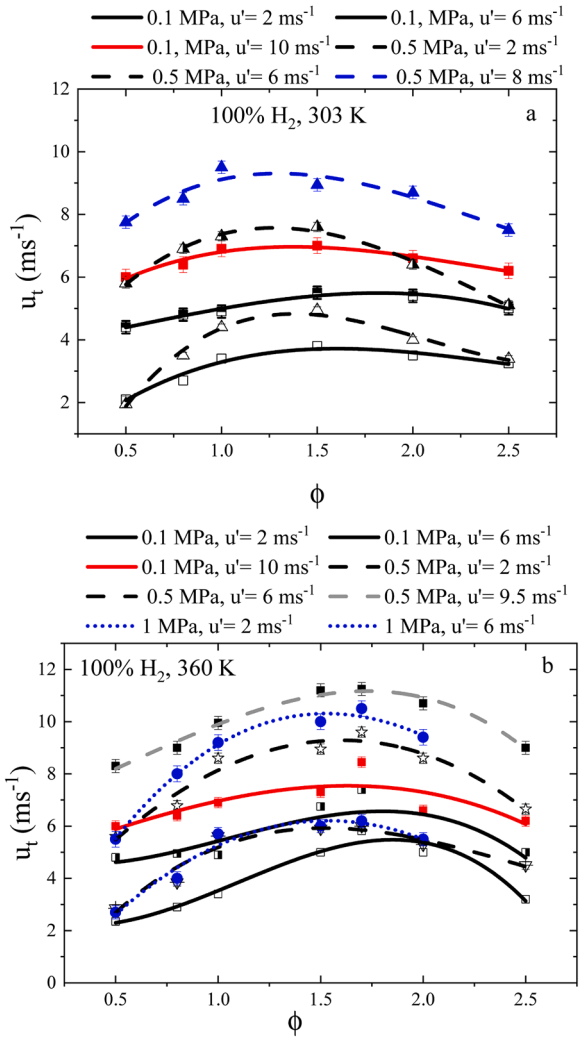

Fig. 11. Variation of turbulent burning velocity at r_v= 30 mm with equivalence ratio for hydrogen flame at different pressures, temperatures and initial rms velocities.

Table 1
The effective rms fluctuation velocity u'_k at r_v= 30 mm for all experimental u'.

u' ms^{-1}	2	6	7.5	8.5	9.5	10
u'_k ms^{-1}	1.409	4.23	5.29	6.0	6.7	7.05

fluctuation turbulent velocity used here is the effective turbulent velocity u'_k which is usually lower than the rms velocity u' depending on the flame radius, (d) the Prandtl number has been included in this correlation as in Eq. (7) (with the present of hydrogen Prandtl number ≠1), and (e) the correlation covered the regime with very low Karlovitz stretch factor (≤ 0.1) which was considered to be unstable in previous studies [2–4].

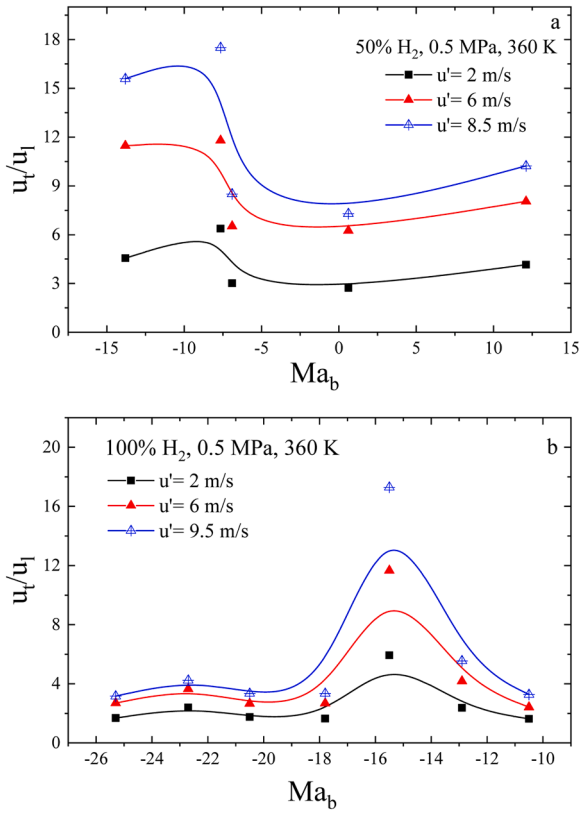

Fig. 12. Variation of normalised turbulent burning velocity with Markstein number Ma_b at 0.5 MPa and 360K (a) 50% H_2 and (b) 100% H_2.

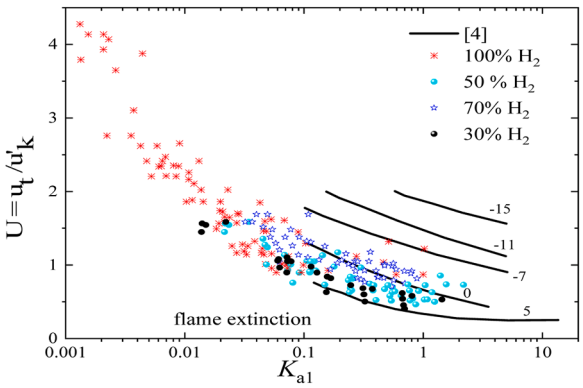

Fig. 13. The present experimental measurements in the *U-K* diagram.

The general scaling parameters from the literature, based on the Damköhler hypothesis, are used to evaluate the current measurements (Fig. 15). The present data seems to be bound around the correlation of

$$\text{For 100\% H2 } \alpha,\ \beta = \begin{cases} \alpha = 0.00175(300 - Ma_b) \pm 0.1, \beta = -0.013(0.1Ma_b + 22) \pm 0.04, \text{ for positive } Ma_b, 0.01 > K_a \leq 0.1 \\ \alpha = 0.00168(300 - Ma_b) \pm 0.1, \beta = -0.015(0.1Ma_b + 22) \pm 0.04, \text{ for negative} Ma_b, K_a \leq 0.01 \end{cases} \quad (9)$$

$$\text{For } \frac{\text{CH4}}{\text{H2}} \alpha,\ \beta = \begin{cases} \alpha = 0.0016(348 - Ma_b) \pm 0.05, \beta = -0.009(Ma_b + 24) \pm 0.05, \text{ for positive } Ma_b, \\ \alpha = 0.0212(348 - Ma_b) \pm 0.03, \beta = -0.01(0.1Ma_b + 22) \pm 0.025, \text{ for negative } Ma_b \end{cases} \quad (10)$$

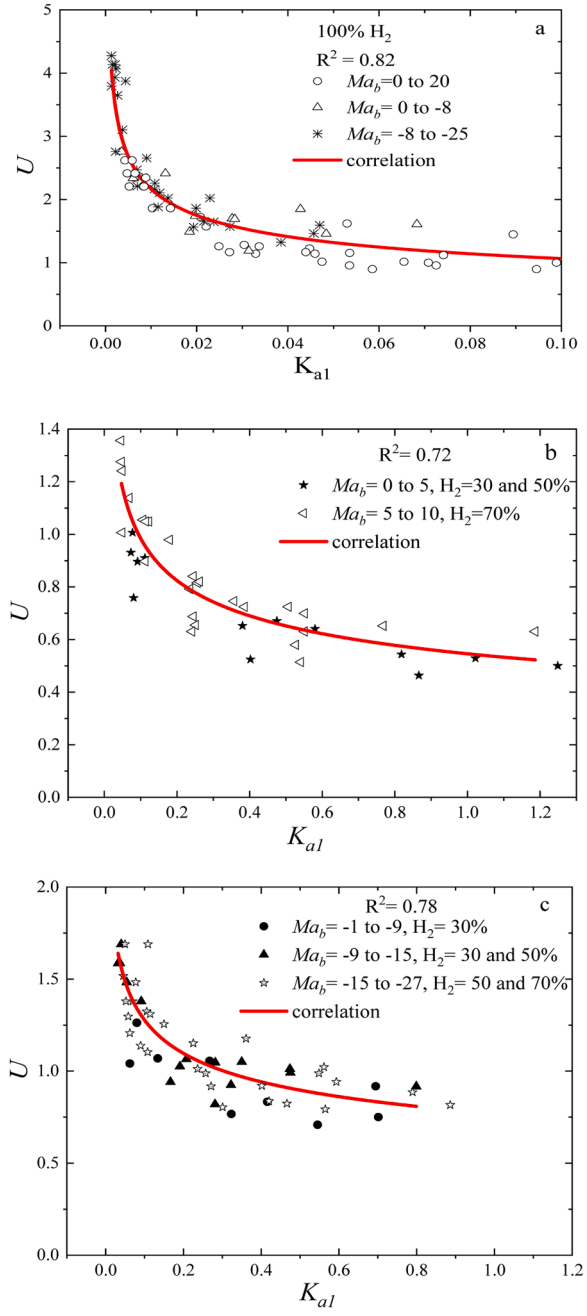

Fig. 14. Correlation of with K_{a1} for different fuel mixtures and Ma_b, (a) pure H_2, Ma_b from -25 to 20, (b) H_2/CH_4, positive Ma_b and (c) H_2/CH_4, negative Ma_b

[13] $\left\{u_t/u_l/K_{a1} = 0.47\ (D_a/Le)^{0.86}\right\}$ with R^2~0.7. The relatively low R^2 value may be due to the present data being spread over a wide range of turbulent regimes (Fig. 1). Therefore, the current data fits better (with R^2=0.85) with the line $\left\{u_t/u_l/K_{a1} = 0.7\ (D_a/Le)^{0.86}\right\}$. This suggests slight differences between the power exponents of the present data and the literature. This difference was also evident in previous studies [13,54], possibly due to the differences in u_t, u_l, δ_l and/or K_{a1}. In addition, the present correlation confirms the previous finding [13] that the performance of general turbulent correlations of the form $\left\{u_t/u_l = (A)^a(B)^b\right\}$ must include any independent parameters A and B from (u'/u_l, L/δ_l, D_a, K_{a1}, R_{eL}) because they are coordinate axes or boundary curves in a combustion regime diagram [55]. Both correlations in Figs. 14 and 15 include at least a pair of these independent parameters. Although both correlations provide good performance in u_t prediction, the scaling

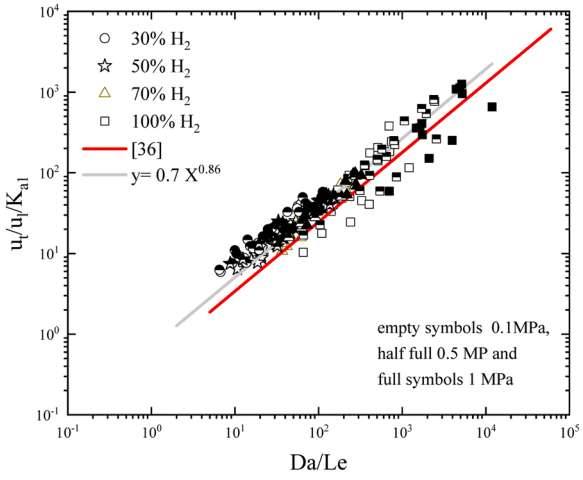

Fig. 15. Normalised turbulent flame speed $u_t/u_l/K_{a1}$ as a function of Da /Le for present data and literature correlation [13].

parameters in Fig. 15 are preferred due to the large uncertainty in the Ma_b values.

4. Conclusions

This study determined turbulent burning velocities for pure hydrogen and methane/hydrogen/air mixtures through spherical flame propagation experiments utilising the Schlieren technique. A broad spectrum of hydrogen volume fractions, equivalence ratios, initial pressures, and rms velocities were explored, particularly under elevated conditions. Several key conclusions can be drawn from our investigation:

- Turbulent burning velocity increases with higher hydrogen volume fractions, elevated fan speeds (u'), and increased temperature. At $u' = 2$ ms^{-1}, variations in initial pressure do not significantly affect u_t; however, for $u' \geq 6$ ms^{-1}, an increase in pressure leads to higher u_t.
- Pure hydrogen flames exhibit short chemical time scales, enabling flame development before the substantial impact of large turbulent eddies. This results in spherical flame propagation with a wrinkled surface.
- The most refined flame wrinkling scales are observed at higher pressures due to reduced turbulent Taylor and extended chemical time scales. An increase in u' reduces the Taylor length scales, leading to finer flame wrinkling scales.
- Flame wrinkling scales are more condensed for 30% H_2 flames than 100% H_2 flames. This is attributed to turbulent eddies having more time to wrinkle the surface in cases with a longer chemical lifetime, as with 30% H_2.
- The normalised turbulent burning velocity peaks within a range of Ma_b values and then flattens to low values as Ma_b becomes more negative, indicating the dominance of laminar burning velocity over turbulence effects (chemical time scales) on u_t for these regions. This influence is also evident in the *U-K* diagram. Therefore, the impact of chemical reactivity takes precedence over the effects of stretch and flame instability. It should be noted that the assertion that positive stretch (negative Ma_b) consistently increases turbulent burning velocity is not universally valid.

Novelty and significance statement

The novelty of this research is the experimental study on the thickened, corrugated and wrinkled flamelet regimes of hydrogen-methane-air mixtures. The turbulent burning velocity of those mixtures has been determined under various conditions (pressure, temperature,

equivalence ratio and rms turbulence velocity) via the classic Schlieren imaging technique. The dimensionless groups (Markstein number and Karlovitz stretch factor) have been proposed for the generic correlation of turbulent burning velocity. It is significant because the existing data on high-pressure turbulent flames, such as one may expect in a hydrogen-fuelled spark-ignition car engine or an industrial gas turbine, are scarce. In addition, the emphasis is put on the study of hydrogen-air flames, and this study is timely given the potential of hydrogen to replace hydrocarbons derived from natural gas and crude oil. Previous experimental studies have limited focus on turbulent flame propagation for hydrogen/air and methane/hydrogen/air mixtures, particularly at high-pressure (10 bar) and high turbulence (u' = 10 ms^{-1}) conditions, which are most relevant to hydrogen-fuelled ICEs and industrial gas turbines and burners. Moreover, this study revisited the previous *U/K* diagram and plotted new data. The latest data is situated in the regime considered unstable in Bradley's earlier studies. In addition, this study provided a new *U-K* correlation based on Ma_b instead of Ma_{sr}. Ma_{sr} is derived for mixtures with a unity Lewis number, which does not apply to the current fuel mixture.

CRediT authorship contribution statement

Marwaan Al-Khafaji: Writing – original draft, Visualization, Validation, Methodology, Investigation, Formal analysis, Data curation. **Junfeng Yang:** Writing – review & editing, Supervision, Resources, Project administration, Funding acquisition, Conceptualization. **Alison S. Tomlin:** Writing – review & editing, Supervision, Formal analysis, Conceptualization. **Harvey M. Thompson:** Writing – review & editing, Supervision, Resources, Funding acquisition, Conceptualization. **Gregory de Boer:** Writing – review & editing, Supervision, Resources, Conceptualization. **Kexin Liu:** Writing – review & editing, Conceptualization.

Declaration of competing interest

The authors declare that they have no known competing financial interests or personal relationships that could have appeared to influence the work reported in this paper.

Acknowledgment

Mr. M. AL-Khafaji acknowledges the Republic of Iraq/ Ministry of Electricity/ State Company of Electricity Production- North region for sponsoring the PhD scholarship. Dr. J. Yang thanks EPSRC (Grant No. EP/W002299/1) for the financial support. Authors would like to acknowledge the valuable discussions with Prof. Derek Bradley and Dr. M.E. Morsy.

Supplementary materials

Supplementary material associated with this article can be found, in the online version, at doi:10.1016/j.combustflame.2024.113907.

References

[1] R.G. Abdel-Gayed, D. Bradley, M. Lawes, Turbulent burning velocities: a general correlation in terms of straining rates, Proc. R. Soc. Lond. Ser. A Math. Phys. Sci. 414 (1987) 389–413.
[2] D. Bradley, M. Lawes, M.S. Mansour, Correlation of turbulent burning velocities of ethanol–air, measured in a fan-stirred bomb up to 1.2 MPa, Combust. Flame 158 (2011) 123–138.
[3] D. Bradley, M. Lawes, K. Liu, M.S. Mansour, Measurements and correlations of turbulent burning velocities over wide ranges of fuels and elevated pressures, Symp. (Int.) Combust. 34 (2013) 1519–1526.
[4] D. Bradley, M. Shehata, M. Lawes, P. Ahmed, Flame extinctions: critical stretch rates and sizes, Combust. Flame 212 (2020) 459–468.
[5] D. Bradley, M.Z. Haq, R.A. Hicks, T. Kitagawa, C.G.W. Sheppard, R. Woolleyet, Turbulent burning velocity, burned gas distribution, and associated flame surface definition, Combust. Flame 133 (2003) 415–430.
[6] H. Kutkan, J. Guerrero, Turbulent pre-mixed flame modeling using the algebraic flame surface wrinkling model: a comparative study between OpenFOAM and ansys fluent, Fluides 6 (2021) 462–481.
[7] H.G. Weller, G. Tabor, A.D. Gosman, C. Fureby, Application of a flame-wrinkling les combustion model to a turbulent mixing layer, Symp. (Int.) Combust. 27 (1998) 899–907.
[8] H. Weller, The Development of a New Flame Area Combustion Model Using Conditional Averaging–Thermo-Fluids Section Report TF, 9307, Imperial College of Science Technology and Medicine, 1993.
[9] E. Yasari, Tutorial XiFoam, Chalmers University of Technology, 2010.
[10] X. Cai, J. Wang, Z. Bian, H. Zhao, M. Zhang, Z. Huang, Self-similar propagation and turbulent burning velocity of CH4/H2/air expanding flames: effect of Lewis number, Combust. Flame 212 (2020) 1–12.
[11] S. Chaudhuri, F. Wu, C.K. Law, Scaling of turbulent flame speed for expanding flames with Markstein diffusion considerations, Phys. Rev. E 88 (2013) 033005.
[12] M. Lawes, M.P. Ormsby, C.G.W. Sheppard, R. Woolley, The turbulent burning velocity of iso-octane/air mixtures, Combust. Flame 159 (2012) 1949–1959.
[13] S. Wang, A.M. Elbaz, G. Wang, Z. Wang, W.L. Roberts, Turbulent flame speed of NH3/CH4/H2/H2O/air-mixtures: effects of elevated pressure and Lewis number, Combust. Flame 247 (2023) 112488.
[14] J. Goulier, A. Comandini, F. Halter, N. Chaumeix, Experimental study on turbulent expanding flames of lean hydrogen/air mixtures, Symp. (Int.) Combust. 36 (2017) 2823–2832.
[15] G. Damköhler, The effect of turbulence on the flame velocity in gas mixtures, NACA-TM, 46 (1947) 1112.
[16] D. Williams D and L. Bollinger, Effect of Reynolds number in turbulent flow range on flame speed of bunsen burner flames, NACA Rep, 932 (1949).
[17] M.S. Mansour, Fundamental study of pre-mixed combustion rates at elevated pressure and temperature, Thesis (Ph.D.), University of Leeds (School of Mechanical Engineering), 2010, Leeds.
[18] M. Al-Khafaji, J. Yang, A. Tomlin, H. Thompson, G. de Boer, K. Liu, M. Morsy, Laminar burning velocities and Markstein numbers for pure hydrogen and methane/hydrogen/air mixtures at elevated pressures, Fuel 354 (2023) 129331.
[19] R. Yu, A.N. Lipatnikov, DNS study of dependence of bulk consumption velocity in a constant-density reacting flow on turbulence and mixture characteristics, Phys. Fluids 29 (2017) 065116.
[20] A. Morones Morones, S. Ravi, D. Plichta, E.L. Petersen, N. Donohoe, A. Heufer, H. J. Curran, F. Güthe, T. Wind, Laminar and turbulent flame speeds for natural gas/hydrogen blends, in: Proceedings of the ASME Turbo Expo 2014: Turbine Technical Conference and Exposition, 4B: Combustion, Fuels and Emissions, 2014 V04BT04A039.
[21] M. Fairweather, M.P. Ormsby, C.G.W. Sheppard, R. Woolley, Turbulent burning rates of methane and methane–hydrogen mixtures, Combust. Flame 156 (2009) 780–790.
[22] M. Nakahara, T. Shirasuna, J. Hashimoto, Experimental study on local flame properties of hydrogen added hydrocarbon pre-mixed turbulent flames, Int. J. Therm. Technol. 4 (2009) 190–201.
[23] R.W. Schefer, Hydrogen enrichment for improved lean flame stability, Int. J. Hydrog. Energy 28 (2003) 1131–1141.
[24] P. Strakey, T. Sidwell, J. Ontko, Investigation of the effects of hydrogen addition on lean extinction in a swirl stabilised combustor, Symp. (Int.) Combust. 31 (2007) 3173–3180.
[25] M. Zhang, J. Wang, Y. Xie, W. Jin, Z. Wei, Z. Huang, H. Kobayashi, Flame front structure and burning velocity of turbulent pre-mixed CH4/H2/air flames, Int. J. Hydrog. Energy 38 (2013) 11421–11428.
[26] B. Karlovitz, D.W. Denniston, D.H. Knapschaefer, F.E. Wells, Studies on turbulent flames: A. flame propagation across velocity gradients B. turbulence measurement in flames, Symp. (Int.) Combust. 4 (1953) 613–620.
[27] R. Yu, A.N. Lipatnikov, DNS study of dependence of bulk consumption velocity in a constant-density reacting flow on turbulence and mixture characteristics, Phys. Fluids 29 (2017) 15.
[28] D. Bradley, M. Lawes, M.E. Morsy, Measurement of turbulence characteristics in a large scale fan-stirred spherical vessel, J. Turbul. 20 (2019) 195–213.
[29] D. Bradley, M. Lawes, M.S. Mansour, The problems of the turbulent burning velocity: computational combustion using high-performance computing, Flow Turbul. Combust. 87 (2011) 191–204.
[30] D. Bradley, R.A. Hicks, M. Lawes, C.G.W. Sheppard, R. Woolley, The measurement of laminar burning velocities and markstein numbers for iso-octane–air and iso-octane–n-heptane–air mixtures at elevated temperatures and pressures in an explosion bomb, Combust. Flame 115 (1998) 126–144.
[31] E. Hu, Z. Huang, J. He, C. Jin, J. Zheng, Experimental and numerical study on laminar burning characteristics of pre-mixed methane–hydrogen–air flames, Int. J. Hydrog. Energy 34 (2009) 4876–4888.
[32] M. Morsy, Studies of laminar and turbulent combustion using particle image velocimetry, Thesis (Ph.D.), University of Leeds (School of Mechanical Engineering), 2019.
[33] C. Morley, Gaseq: a chemical equilibrium program for Windows, ed, 2005.
[34] W.D. McComb, The Physics of Fluid Turbulence, Oxford University Press, 1990.
[35] R. Borghi, On the structure and morphology of turbulent pre-mixed flames, in: C. Casci, C. Bruno (Eds.), Recent Advances in the Aerospace Sciences: In Honor of Luigi Crocco on his Seventy-Fifth Birthday, Springer US, Boston, MA, 1985, pp. 117–138.
[36] N. Peters, Laminar flamelet concepts in turbulent combustion, Symp. (Int.) Combust. 21 (1988) 1231–1250.
[37] R.G. Abdel-Gayed, D. Bradley, M.N. Hamid, M. Lawes, Lewis number effects on turbulent burning velocity, Symp. (Int.) Combust. 20 (1985) 505–512.

[38] T. Poinsot, D. Veynante, S. Candel, Quenching processes and pre-mixed turbulent combustion diagrams, J. Fluid Mech. 228 (1991) 561–606.
[39] S.B. Pope, Turbulent pre-mixed flames, Ann. Rev. Fluid Mech. 19 (1987) 237–270.
[40] F. Zhang, H. Bonart, T. Zirwes, P. Habisreuther, H. Bockhorn, N. Zarzalis, Direct numerical simulation of chemically reacting flows with the public domain code OpenFOAM, in: W. Nagel, D. Kröner, M. Resch (Eds.), High Performance Computing in Science and Engineering '14, Springer, Cham, 2014, pp. 221–236, c.
[41] X. Qin, H. Kobayashi, T. Niioka, Laminar burning velocity of hydrogen–air pre-mixed flames at elevated pressure, Exp. Therm. Fluid Sci. 21 (2000) 58–63.
[42] M.E. Morsy, J. Yang, The instability of laminar methane/hydrogen/air flames: correlation between small and large-scale explosions, Int. J. Hydrog. Energy 47 (2022) 29959–29970.
[43] D. Bradley, P.H. Gaskell, X.J. Gu, A. Sedaghat, Pre-mixed flamelet modelling: factors influencing the turbulent heat release rate source term and the turbulent burning velocity, Combust. Flame 143 (2005) 227–245.
[44] K.N.C. Bray, R.S. Cant, Some applications of Kolmogorov's turbulence research in the field of combustion, Proc. R. Soc. A Math. Phys. Sci. 434 (1890) 217–240, 1991.
[45] M. Allard, L. Chatelier, Recherches sur la combustion des mélanges gazeux explosifs, J. Phys. Theor. 84 (1985) 59–84.
[46] G.S. Jackson, R. Sai, J.M. Plaia, C.M. Boggs, K.T. Kiger, Influence of H2 on the response of lean pre-mixed CH4 flames to high strained flows, Combust. Flame 132 (2003) 503–511.
[47] E. Salzano, F. Cammarota, A. Di Benedetto, V. Di Sarli, Explosion behavior of hydrogen–methane/air mixtures, J. Loss Prev. Process Ind. 25 (2012) 443–447.
[48] D. Bradley, A.K.C. Lau, M. Lawes, F.T. Smith, Flame stretch rate as a determinant of turbulent burning velocity, Philos. Trans. R. Soc. Lond. Ser. A Phys. Sci. Eng. 338 (1992) 359–387.
[49] K.N.C. Bray, Turbulent combustion. By Norbert Peters Cambridge University Press, 2000. 320 pp. ISBN 0521 60823, J. Fluid Mech. 426 (2001) 407–409.
[50] H. Kobayashi, Y. Kawabata, K. Maruta, Experimental study on general correlation of turbulent burning velocity at high pressure, Symp. (Int.) Combust. 27 (1998) 941–948.
[51] T.L. Howarth, A.J. Aspden, An empirical characteristic scaling model for freely-propagating lean pre-mixed hydrogen flames, Combust. Flame 237 (2022) 111805.
[52] D. Bradley, P.H. Gaskell, X.J. Gu, Burning velocities, markstein lengths, and flame quenching for spherical methane-air flames: a computational study, Combust. Flame 104 (1996) 176–198.
[53] X.J. Gu, M.Z. Haq, M. Lawes, R. Woolley, Laminar burning velocity and Markstein lengths of methane–air mixtures, Combust. Flame 121 (2000) 41–58.
[54] T. Kitagawa, T. Nakahara, K. Maruyama, K. Kado, A. Hayakawa, S. Kobayashi, Turbulent burning velocity of hydrogen–air pre-mixed propagating flames at elevated pressures, Int. J. Hydrog. Energy 33 (2008) 5842–5849.
[55] V.A. Sabelnikov, A.N. Lipatnikov, Bifractal nature of turbulent reaction waves at high Damköhler and Karlovitz numbers, Phys. Fluids 32 (2020) 095118.